The Effect of Welding Procedure on ANSI/AWS A5.29-98 E81T1-Ni1 Flux Cored Arc Weld Metal Deposits

Arc energy, number of passes per layer, welding position, and shielding gas type were considered

BY H. G. SVOBODA, N. M. RAMINI DE RISSONE, L. A. DE VEDIA, AND E. S. SURIAN

ABSTRACT. The objective of this work was to study the effects that different shielding gases (CO_2 and a mixture of 80% Ar/20%CO_2), welding position (flat and uphill), arc energy (1.0 vs. 1.9 kJ/mm) and number of passes per layer (two and three) have on the all-weld-metal microstructure and mechanical properties of an ANSI/AWS A5.29-98 E81T1-Ni1 flux cored wire, 1.2 mm diameter. Hardness, tensile, and impact tests were used to assess the mechanical properties, and quantitative metallographic analyses were performed to identify the resulting microstructures. In general, ANSI/AWS A5.29-98 E81T1-Ni1 (E81T1-Ni1M) mechanical requirements were comfortably satisfied under Ar/CO_2, but significant variations were found with different welding procedures. These variations have been rationalized in terms of the microstructure and chemical composition of the weld deposits. The strength and toughness of welds produced with Ar/CO_2 were quite sensitive to minor changes in heat input, while the CO_2 welds exhibited little deviation in these properties with nearly identical changes in heat input.

Introduction

During the last twenty to thirty years, there has been a worldwide trend toward replacing shielded metal arc welding using flux covered electrodes with other processes that have higher deposition rates and lend themselves to automation (Ref. 1). In spite of some negative features, the shielded metal arc process (Ref. 2) will not be completely replaced in the foreseeable future, but it is estimated that approximately 70% of the deposited weld metal will come from more efficient processes in the future. Continuous wires are increasingly used, and among them, flux and metal cored wires. These welding consumables are very versatile because relatively small quantities of electrodes can be produced with a wide variety of weld deposits and different chemical compositions, which exhibit adequate mechanical properties for all-position welding (Refs. 3–5). Among the different cored wire types, those using gas protection are flux cored and metal cored wires. They present different characteristics, advantages, and disadvantages. It is known that flux cored wires provide improved joint penetration, smooth arc transfer, low spatter levels, and, most important, are easier to use than solid wires (Refs. 6, 7). It is also possible to achieve high deposition rates (Refs. 6, 7) with them.

On the other hand, it is well known that the employment of different shielding gases as well as changes in the welding procedure parameters lead to variations in the deposit characteristics (Refs. 8–15). Generally, the most frequently used gas for welding with rutile-type flux cored wires is CO_2, but it is also possible to use Ar/CO_2 mixtures. This type of mixture results in improved appearance, less spatter, and better arc stability (Ref. 8). On the other hand, in all arc welding processes, the arc energy influences metallurgical transformations and resulting mechanical properties and microstructure (Refs. 9–13), so it is very important to control it. In multipass welding, changes in welding parameters lead to different arc energies and different numbers of passes per layer for the same joint design (Refs. 9, 10). The welding position is another important variable (Ref. 16). The objective of this work was to study the effect of shielding gas type (CO_2 and Ar/CO_2 mixture), flat and uphill welding positions, arc energy, and number of passes per layer (two and three) on the all-weld metal mechanical properties and microstructure obtained from ANSI/AWS A5.29-98 E81T1-Ni1 flux cored wire.

H. G. SVOBODA is with Metallographic Laboratory, Mechanical and Navy Engineering Department, Faculty of Engineering, University of Buenos Aires, Argentina. N. M. RAMINI DE RISSONE is with DEYTEMA-Materials Developments and Technology Center, Regional Faculty of San Nicolas, National Technological University, San Nicolas, Buenos Aires, Argentina. L. DE VEDIA is with Institute of Technology Jorge A. Sabato, National University of San Martin-National Commission of Atomic Energy, CIC, Buenos Aires, Argentina. E. S. SURIAN is with Research Secretary, Faculty of Engineering, National University of Lomas de Zamora, Buenos Aires and DEYTEMA-Materials Development and Technology Center, Regional Faculty of San Nicolas, National Technological University, San Nicolas, Buenos Aires, Argentina.

KEY WORDS

Flux Core
Gas Shielding
FCAW
CO_2
Ar/CO_2
Charpy V-Notch
Tensile Strength

Experimental Procedure

Weldments/Electrodes

The consumable employed in this work was a commercial product that, according to the manufacturer, is classified as ANSI/AWS A5.29-98 (Ref. 17) E81T1-Ni1 flux cored wire, in 1.2-mm diameter.

Test Specimens

With this wire, eight all-weld-metal test coupons were prepared for flat welding according to ANSI/AWS A5.29-98 standard (Ref. 17), which is shown in Fig. 1A. The preparation included the following:

1) Two shielding gases: pure CO_2 and a mixture of 80% Ar-20% CO_2 (Ar/CO_2).

2) Two arc energies: high (two beads per layer) and low (three beads per layer).

3) Flat and uphill welding positions.

The key to the identification of the weld test specimens is C means welding under CO_2 and A welding under Ar/CO_2 shielding; 2 and 3 represent the number of passes per layer; while F and V the flat and uphill welding positions, respectively. Welding parameters employed are shown in Table 1.

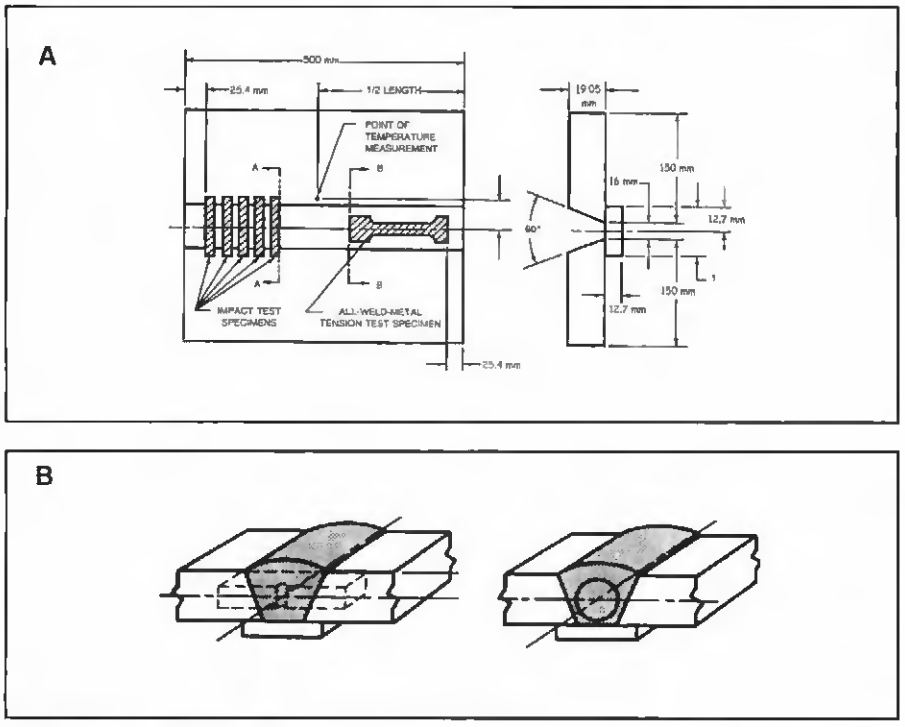

Fig. 1 — A — Location of test specimens in plan view (left) and cross section showing joint preparation (right); B — location of impact and tensile test specimens in perspective.

Table 1 — Welding Parameters Used for the All-Weld-Metal Test Coupons

Weld	Protection Type	No. Passes per Layer	No. Layers	Intensity (A)	Tension (V)	Welding Speed (mm/s)	Heat Input (kJ/mm)
C2F	CO_2	2	6	230	30	4.4	1.8
C3F	CO_2	3	6	195	28	4.8	1.3
A2F	Ar/CO_2	2	6	210	28	3.3	1.9
A3F	Ar/CO_2	3	6	200	27	5.2	1.2
C2V	CO_2	2	6	170	23	2.5	1.7
C3V	CO_2	3	6	153	21	3.1	1.2
A2V	Ar/CO_2	2	6	170	22	2.3	1.9
A3V	Ar/CO_2	3	6	154	21	3.4	1.0
AWS req.[a]		2 or 3	5 to 8	NS	NS	NS	NS

Coupons were welded in the flat and uphill positions with different gas shielding.
Preheating temperature was 150°C. Interpass temperature was in the range of 140–150°C. The plates were buttered with the same electrode used as filler metal and preset to avoid excessive distortion. Electrode extension was 20 mm in all cases.
Gas flow: 20 L/min. NS: not specified. (a): only for flat welding position.

Tensile and Impact Tests and Hardness Measurements

From each all-weld-metal test coupon, a minitrac (Ref. 18) tensile specimen was extracted (total length = 55 mm, gauge length = 25 mm, reduced section diameter = 5 mm, gauge length-to-diameter ratio = 5:1), and enough Charpy specimens with the V notch located as shown in Fig. 1B were machined to construct an absorbed energy vs. test temperature curve between –80°C (–112 °F) and 20°C (68°F). A cross section was also obtained from each specimen to conduct a microhardness survey, at the Charpy V-notch location, using a 1000-g load and metallographic analysis. Tensile tests and Charpy impact tests were performed in the as-welded condition. Prior to testing at room temperature, tensile specimens were heat-treated for 24 h at 200°C (328°F) to eliminate hydrogen.

Chemical Composition

All-weld-metal spectrometric chemical analyses were conducted on a cross section of each weld coupon. Nitrogen and oxygen determinations were made with LECO equipment that extracted the samples from the broken ends of the tensile specimens.

Metallographic Study

Examination of cross sections (etched with Nital 2%) was carried out in the top heads and the Charpy V-notch location (Fig. 2), as described previously (Ref. 19). The area fraction of columnar and weld metal reheated zones were measured at 500× at the Charpy V-notch location. The average width of the columnar grain size (prior austenite grains) was measured in the top bead of the samples at 100×. To quantify the microstructural constituents of the columnar zones in each weld, 10 fields of 100 points were measured in the top head at 500× by light microscopy. The reheated fine-grained size was measured in the heat-affected zone of the top bead, according to the linear intercept method, ASTM E112 standard (Ref. 20).

Results and Discussion

All-Weld Metal Chemical Composition

Table 2 presents the all-weld-metal chemical composition. A marked variation in the oxygen levels was observed, with higher values in the welds made with CO_2 protection. Due to this difference, carbon, manganese, and silicon values were lower for this type of gas. Nitrogen values were very low, as well as residual elements such as P, S, Cr, Mo, V, Co, Cu, and Al showing a very clean weld deposit. No influence of the heat input was detected (two or three passes per layer). Considering the chemical composition under Ar/CO_2, the AWS requirements were satisfied.

It has been shown (Ref. 5) that when the same wire is used with the Ar/CO_2 gas mixture instead of pure CO_2, the O content in the gas mixture, which originates from the decomposition of CO_2, decreases, as well as the O partial pressure in the arc. With Mn and Si being deoxidants in addition to alloying elements, a smaller amount of these elements will be oxidized under Ar/CO_2 than under CO_2, leading to a higher recovery of them in the weld metal.

Metallographic Analysis

General

Table 3 shows the area fraction of columnar and reheated coarse- and fine-grained zones (HAZ), corresponding to the Charpy V-notch location. It was seen that the proportion of columnar zones was always larger in samples welded with

lower arc energy (three passes per layer) as previously found (Refs. 9, 10, 21, 22). This observation is mainly related to the geometrical distribution of the weld beads in relation to the location of the Charpy V-notch and the relative increment of the columnar zone with respect to the reheated zone when heat input is reduced (Ref. 22).

When compared to the samples welded in the flat position, those welded in the uphill position presented a larger proportion of columnar zones, as shown by Evans (Ref. 16) for shielded metal arc weld deposits of the ANSI/AWS A5.1-91 E7018 type, and smaller amount of fine-grained recrystallized zones as found previously (Ref. 22). The largest proportion of reheated zones and within these the largest amount of fine-grained recrystallized zones were found in the welds welded in the flat position under Ar/CO_2 shielding.

Columnar Zone — As-Welded

Table 4 shows the percentages of microconstituents present in the columnar zone of the last bead of each weld. A lower proportion of acicular ferrite (AF), a higher amount of grain boundary primary ferrite (PF[G]), along with a higher proportion of intragranular primary ferrite (PF[I]) and higher ferrite content with second phase, aligned (FS[A]) and not aligned (FS[NS]), were found for CO_2 shielding than for the Ar/CO_2 gas mixture. No effect of the variation of heat input was detected. The higher amount of PF(G) found in the coupons welded under CO_2 may be related to the corresponding higher oxygen content in the weld metal that could increase the amount of inclusions present in the primary grain boundaries that acted as nucleation sites for grain boundary ferrite (Refs. 23, 24). Additionally, the C, Mn, and Si contents in the CO_2 welds were lower than in Ar/CO_2 welds, reducing the hardenability of the weld metal and increasing the proportion of PF(G).

Table 4 also shows the average columnar grain widths, which were measured only in deposits obtained under CO_2 shielding due to the very low amount of grain boundary ferrite in welds made under Ar/CO_2. For both welding positions, it was observed that lower values of prior austenite grain size were achieved for lower heat inputs, as found previously (Refs. 9, 10, 22).

Reheated Zones (HAZ)

The results from the measurements of the fine-grained size of the reheated zone (HAZ) are also presented in Table 4. For flat welding position, a smaller reheated zone fine-grained size could be seen in deposits welded under Ar/CO_2. In the uphill welding position, no differences were found. Figure 4 shows the microstructure of these regions where this effect can be observed.

Table 2 — All-Weld-Metal Chemical Composition

Sample	C2F	C3F	A2F	A3F	C2V	C3V	A2V	A3V	E81T1-Ni1
C	0.040	0.033	0.047	0.045	0.037	0.042	0.048	0.050	0.12 max.
Si	0.17	0.17	0.28	0.32	0.26	0.24	0.33	0.35	0.80 max.
Mn	1.12	1.08	1.39	1.47	1.35	1.30	1.50	1.53	1.50 max.
P	0.005	0.005	0.005	0.005	0.005	0.005	0.005	0.005	0.03 max.
S	0.009	0.009	0.009	0.010	0.009	0.009	0.009	0.010	0.03 max.
Cr	0.03	0.03	0.03	0.03	0.03	0.03	0.03	0.03	0.15 max.
Mo	<0.01	<0.01	<0.01	0.03	0.03	0.03	0.03	0.03	0.35 max.
Ni	0.83	0.78	0.81	0.81	0.80	0.83	0.79	0.81	0.80–1.10
Al	0.01	0.01	0.01	0.01	0.01	0.01	0.01	0.01	NS
Co	0.016	0.014	0.013	0.013	0.012	0.013	0.013	0.013	NS
Cu	0.04	0.04	0.04	0.04	0.04	0.04	0.04	0.04	NS
V	0.013	0.015	0.014	0.014	0.014	0.015	0.015	0.015	0.05 max.
N	33	23	21	27	23	20	22	19	NS
O	548	572	485	458	526	517	467	515	NS
Heat input (kJ/mm)	1.8	1.3	1.9	1.2	1.7	1.2	1.9	1.0	NS

NS: not specified.
All the elements in wt-%, except O and N, which are in ppm.

Table 3 — Percentage of Columnar and Reheated Zones at the Charpy V-Notch Location

Weld	Heat Input (kJ/mm)	Reheated Weld Metal (%)		Primary Weld Metal (columnar) (%)
		HAZ-CG	HAZ-FG	
C2F	1.8	9	66	25
C3F	1.3	23	48	29
A2F	1.9	10	78	12
A3F	1.2	10	75	15
C2V	1.7	23	48	29
C3V	1.2	16	43	41
A2V	1.9	18	23	59
A3V	1.0	15	12	73

HAZ-CG: Heat-affected zone coarse grain
HAZ-FG: Heat-affected zone fine grain

Mechanical Properties

Hardness

Table 5 presents the microhardness values obtained in the columnar, coarse, and fine reheated zones, as well as the weighted averages. As a general tendency, columnar and coarse-grained reheated zones presented similar hardness values, but higher than the fine-grained reheated zone. Deposits welded under Ar/CO_2 shielding presented higher HAZ-FG, HAZ-CG, columnar zone, and weighted average values than under

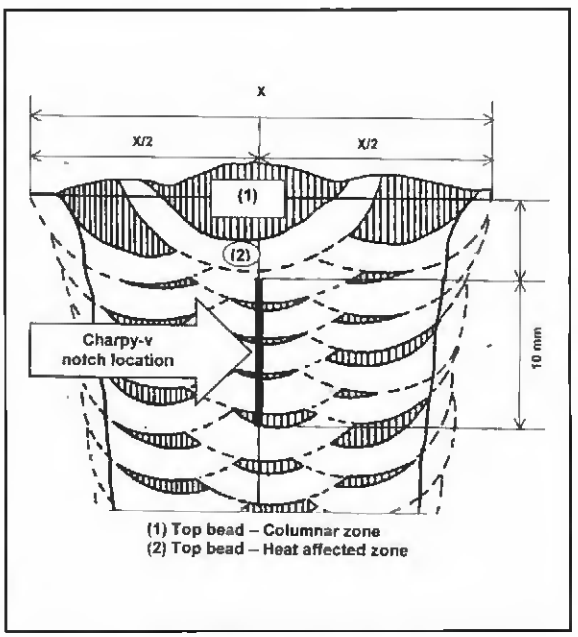

Fig. 2 — Cross section of the all-weld-metal test assembly.

Table 4 — Microconstituents and Primary Austenitic Grain Size

Weld	Heat Input (kJ/mm)	AF %	PF(G) %	PF(I) %	PF %	FS(NA) %	FS(A) %	FS %	HAZ-FG (μm)	Average Columnar Grain Width (μm)
C2F	1.8	9	42	11	53	31	7	38	5.6	156
C3F	1.3	8	42	10	52	36	4	40	6.2	134
A2F	1.9	17	2	21	23	47	13	60	4.8	(a)
A3F	1.2	24	5	17	22	49	5	54	4.7	(a)
C2V	1.7	16	25	6	31	52	1	53	4.2	176
C3V	1.2	19	30	7	37	42	2	44	3.9	105
A2V	1.9	18	9	16	25	48	9	57	4.3	(a)
A3V	1.0	20	9	9	18	41	21	62	4.3	(a)

AF: acicular ferrite. PF(G): Grain boundary primary ferrite. PF(I): Intragranular primary ferrite. FS(NA): Ferrite with nonaligned second phases. FS(A): Ferrite with aligned second phases. HAZ-FGS: Heat-affected zone fine-grain size.
(a) It was not possible to measure this due to very low level of PF(G).

Table 5 — Vickers Microhardness Measurements (1000 g)

Zone	C2F	C3F	A2F	A3F	C2V	C3V	A2V	A3V
HAZ-FG	167	175	191	196	187	194	195	220
HAZ-CG	177	180	216	213	199	215	210	252
Columnar zone	187	193	221	218	207	215	216	248
Weighted average	175	184	204	208	199	210	207	243
Heat input (kJ/mm)	1.8	1.3	1.9	1.2	1.7	1.2	1.9	1.0

HAZ-FG: Heat-affected zone fine grain. HAZ-CG: Heat-affected zone coarse grain.

CO_2 protection. The weighted average hardness values found in all samples welded with lower heat input, three passes per layer, were higher than those obtained with two passes per layer, as was expected (Ref. 11).

Tensile Properties

Table 6 shows tensile test results. In accordance with the results of both chemical composition and hardness measurements, tensile and yield strengths of deposits welded under Ar/CO_2 were higher than those obtained under CO_2 shielding, probably due to higher Mn and Si values as a result of lower weld metal oxygen contents. As a general trend, in welds deposited with two passes per layer (higher heat input), these properties were lower than with three passes per layer (lower heat input), as was expected due to the softening of the weld metal (Refs. 9, 10, 11, 12, 21). For both types of gas shielding, tensile and yield strengths were higher in the uphill welding position. In welds made with Ar/CO_2 shielding, a noticeable effect of heat input was a marked increase in tensile and yield strengths for welds made with three passes per layer (lower heat input). In welds made under CO_2, no significant effect from heat input was detected. Elongation values were very high, exceeding in all cases the requirements of the corresponding AWS standard. Under Ar/CO_2 protection, the ANSI/AWS A5.29-98 E81T1-Ni1 tensile requirements were comfortably satisfied.

Charpy V-Notch Impact Properties

The values of absorbed energy for each test temperature in the Charpy V-notch tests are presented in Table 7. Figures 5 and 6 show the absorbed energy vs. testing temperature for each gas shielding type. Table 8 shows the testing temperatures corresponding to 50 J and 100 J of absorbed energy for each weld.

These welds were very sensitive to welding procedure variations. The best impact properties at low temperatures, particularly at –60°C, were achieved under the Ar/CO_2 mixture, with two and three passes per layer in the flat welding position, and under CO_2 in the uphill position also with two and three passes per layer. The outstanding low-temperature impact behavior for the A2F and A3F welds can be explained by the fact that these deposits presented the lowest O content, intermediate Mn level, the lowest proportion of columnar zone, the highest AF volume fraction, the lowest amount of PF(G) in the columnar zone, and the highest fine-grained recrystallized zone. The A2F weld deposit that presented the best impact properties (on average 120 J at –80°C) also showed the highest percentage of fine-grain reheated zone.

The excellent impact properties in the uphill welds made with CO_2 shielding for both heat inputs can be explained by the intermediate Mn content between 1.3% and 1.4%. In this respect, it is worth noting that weld A3F showed at –60°C somewhat lower impact values than A2F, C2V, and C3V welds. This difference in impact behavior can be the result of weld A3F having a slightly higher Mn level (1.47% Mn) than the other mentioned welds (1.3–1.4% Mn). This difference in impact properties becomes more marked at –80°C. A Mn level between 1.2 and 1.4% was signaled as the optimum by Evans (Ref. 25) to achieve the best impact properties at low temperature in 1% Ni-bearing welds. Figure 7 shows the impact values obtained at –80°C as a function of the Mn content where the optimum Mn level is between 1.3% and 1.4% (Ref. 25).

Additionally, C2V and C3V welds presented the lowest recrystallized fine-grained size, and in particular weld C3V showed the smaller prior austenite average grain width, which is consistent with weld C3V presenting higher impact values than C2V, particularly at –80°C. It is worth noting that very good impact values were obtained with C2V and C3V deposits, notwithstanding that these welds had a relatively low proportion of AF, and a relatively high content of PF(G). This fact points to the limitations of explaining the mechanical behavior of multipass weld deposits in terms of the microstructure of the last bead, since this is not necessarily representative of the microstructure in the region where the notch of the Charpy V specimen is located.

C2F and C3F deposits showed the lowest impact properties at low temperatures. They presented the lowest contents of both AF and Mn, which is consistent with the effect that Mn has in promoting formation of AF. Besides, these welds had the highest proportion of PF(G), leading to a reduction of tensile properties and hardness values. As a general trend in welds made under Ar/CO_2 shielding for both welding positions, a marked reduction in toughness was found in welds made with three passes per layer (lower heat input). In welds made under CO_2, a much smaller effect of heat input on toughness was detected.

Table 9 shows the values of absorbed energy at –29 °C. It can be seen that for any welding condition, the AWS requirement of 27 J on average for this temperature, was comfortably satisfied. There was not a single value under the required minimum.

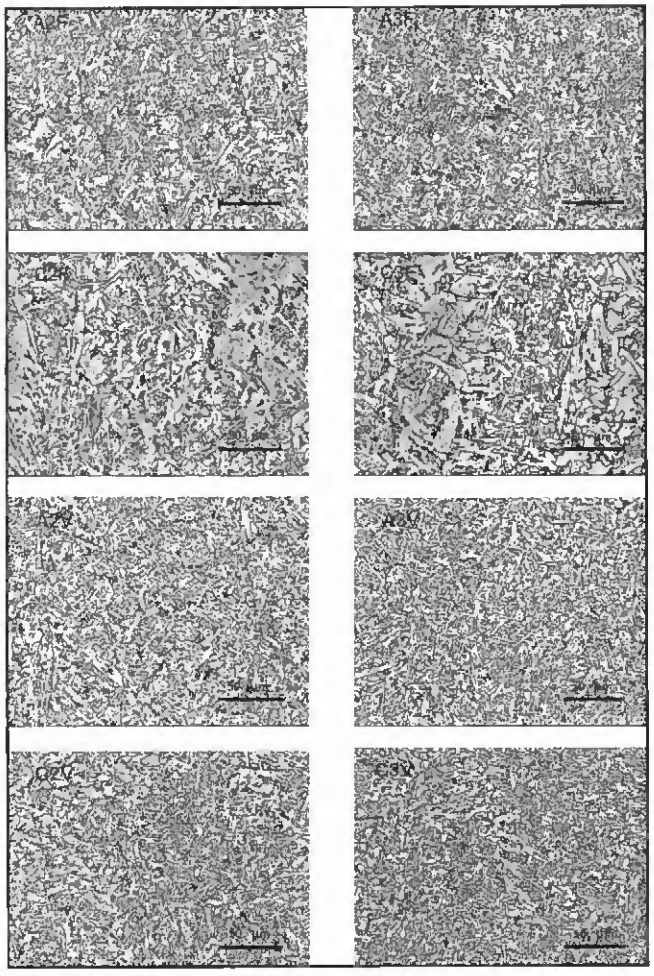

Fig. 3 — Typical columnar zones of different weld deposits.

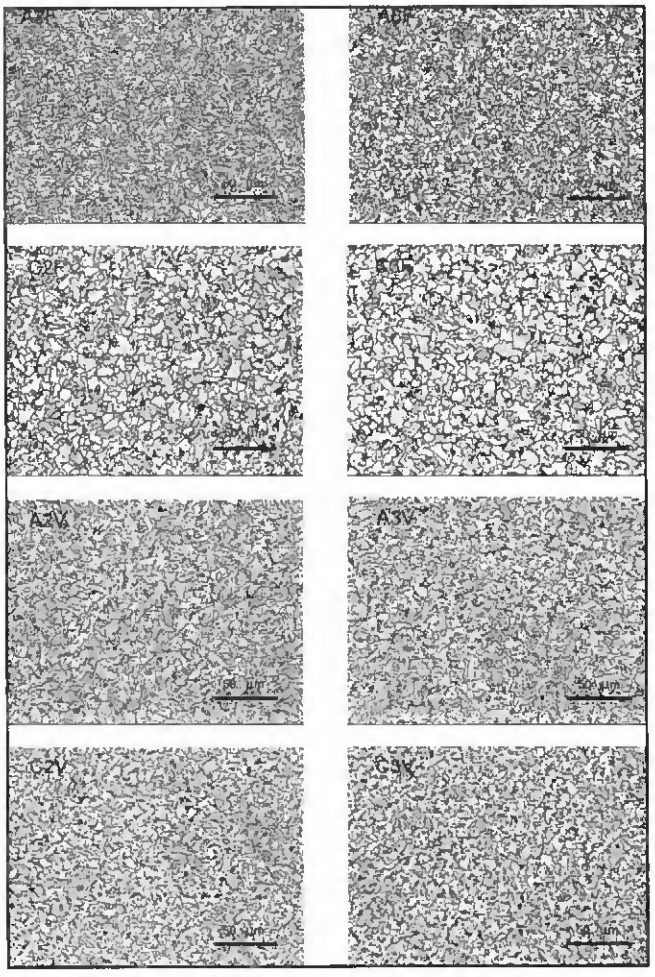

Fig. 4 — Reheated zones.

In spite of having found differences in the toughness values for the different welding conditions, the consumable object of this work presented excellent impact properties for all the temperature range considered and for all the conditions studied.

As a final remark, the importance of matching the shielding gas to the consumable should be emphasized, since using Ar/CO_2 shielding gas and consumables designed for use with 100% CO_2 may result in richer-than-expected deposits, which may or may not meet the anticipated mechanical properties.

Table 6 — All-Weld-Metal Tensile Properties

Properties	C2F	C3F	A2F	A3F	C2V	C3V	A2V	A3V	Req. AWS E81T1-Ni1[a]
UTS (MPa)	507	497	572	619	554	560	598	694	550–690
YS (MPa)	425	424	490	538	483	487	507	642	470 min.
e (%)	30	26	25	24	25	26	21	18	19 min.
A (%)	77	76	79	75	77	73	73	73	NR
Heat input (kJ/mm)	1.8	1.3	1.9	1.2	1.7	1.2	1.9	1.0	NR

UTS: ultimate tensile strength, YS: yield strength, e: elongation, A: reduction in area.
(a) E81T1-Ni1 classification requires CO_2 protection and E81T1-Ni1M requires 75-80/Ar/balanceCO_2 protection.

Conclusions

In all-weld-metal samples produced with 1.2-mm-diameter ANSI/AWS A5.29-98 E81T1-Ni1 flux cored electrode using CO_2 and Ar/CO_2 shielding, in the flat and uphill welding positions, with high arc energy (two passes per layer) and low arc energy (three passes per layer), the following was found:

- The all-weld-metal test specimens welded under CO_2 presented lower levels of C, Mn, and Si and higher oxygen contents. Carbon, Mn, and Si were also lower in the flat welding position for both shielding gases. Nitrogen contents were all very low. Silicon contents of welds made under CO_2 in the flat position were the lowest.
- For both shielding gases, columnar zone percentages were higher for three passes per layer (lower heat input) and the uphill position.
- Under CO_2 shielding, average columnar grain widths were lower with three passes per layer (lower heat input). Under Ar/CO_2, it was not possible to perform this measurement due to the absence of PF(G).
- In the columnar zones of welds made under CO_2, the AF volume fraction was lower and PF(G) volume fraction was higher than in those made under Ar/CO_2.

Table 7 — All-Weld-Metal Charpy-V Impact Test Results (J)

T (°C)	C2F	C3F	A2F	A3F	C2V	C3V	A2V	A3V
20	186-206-214	170-184-194	170-185	144-144-146	154-164-156	162-160-156	134-132-136	96-97-107
	202	183	178	145	158	159	134	100
0	179-197-206	196-179-194	194-194-207	137-138-119	172-165-160	167-157-182	138-130-122	87-100-82
	194	183	198	131	166	169	130	90
–20	159-174-180	159-147-147	185-174-202	127-134-124	181-167-172	142-159-163	100-99-119	61-83-79
	171	151	187	128	173	155	106	74
–40[a]	130-158-130	132-87-82	134-121-148	125-105-132	134-136-130	130-145-140	97-105-106	58-60-50
	139	100	134	121	133	138	103	56
–60	60-90-102	72-69-25	135-122-134	119-78-127	116-97-137	128-120-128	56-79-55	25-26-44
	84	55	130	102	117	125	63	32
–80	19-16-13	15-13-12	117-124-120	45-41-49	92-69-73	89-113-124	44-46-63	46-40-59
	16	13	120	45	78	109	51	48

The values in the upper line correspond to measurements and the single values in the lower line are their averages.
(a) Req. AWS, –29°C 27 J

Table 8 — 50 and 100 J Absorbed Energy Transition Temperatures

	C2F	C3F	A2F	A3F	C2V	C3V	A2V	A3V
50 J, T (°C)	–70	–60	<–80[a]	–79	<–80	<–80[a]	–79	–43
100 J, T (°C)	–55	–42	<–80[a]	–59	–67	<–80[a]	–34	>20

(a) At the minimum test temperature employed (–80°C), it absorbed 120 J on average.
(b) At the minimum test temperature employed (–80°C), it absorbed 109 J on average.

Table 9 — Charpy-V Absorbed Energy in J at –29°C

	C2F	C3F	A2F	A3F	C2V	C3V	A2V	A3V	AWS req.
–29°C	158	134	175	130	155	148	104	61	27 J min.

–29°C is the AWS test temperature requirement.

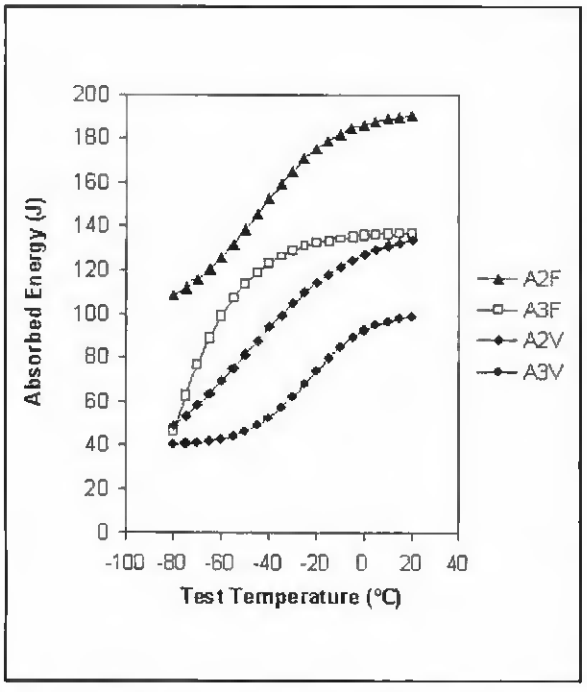

Fig. 5 — Charpy-V notch impact results for all-weld-metals Ar/CO_2 protection.

Reheated zone fine-grain sizes were larger in the flat welding position and under CO_2.

• Hardness in specimens welded under CO_2 was lower than specimens made using Ar/CO_2 mixture. A similar effect was found with two passes per layer (higher heat input) when compared to specimens with three passes per layer (lower heat input). Hardness values of columnar zones were higher than in the reheated zones, and among these last zones, values corresponding to HAZ-CG regions were higher than those of the HAZ-FG regions.

• Tensile properties were higher in welds made under Ar/CO_2 mixture and with three passes per layer (lower heat input), in correlation to chemical composition and hardness results.

• With Ar/CO_2 shielding, impact values were higher in the flat welding position and with two passes per layer (higher heat input).

• With CO_2 shielding, the best toughness was obtained in the uphill welding position, but the results were very close for all the welding conditions used with this gas.

• Considering all the welding conditions, the best impact values were achieved in the flat welding position with two passes per layer (higher heat input) and under Ar/CO_2, and the lowest values were obtained with the same shielding gas, in the uphill welding position, and three passes per layer (lower heat input).

• The strength and toughness of welds produced with Ar/CO_2 were quite sensitive to minor changes in heat input, while the CO_2 welds exhibited little deviation in these properties with nearly identical changes in heat input.

• ANSI/AWS A5.29-98 E81T1-Ni1 (E81T1-Ni1M) requirements were comfortably satisfied under Ar/CO_2.

Acknowledgments

The authors wish to express their gratitude to Air Liquide Argentina S.A. for supplying the consumables and the facilities for the production of the welds; to the Centre Téchnique des Applications du Soudage, Air Liquide France, for conducting nitrogen and oxygen determinations; to Conarco-ESAB Argentina for carrying out the chemical analysis; and to the Fundación Latinoamericana de Soldadura, Argentina, for the facilities provided to weld and for machining and mechanical testing. Authors recognize ANPCyT, Argentina, for the financial support.

References

1. Myazaki, T. 1989. Flux cored wires for robots. IIW-IIS Doc XII-1084-88. Hitachi Zosen Corporation, Ariabe Works.

2) Ferree, S. E. 1995. New generation of

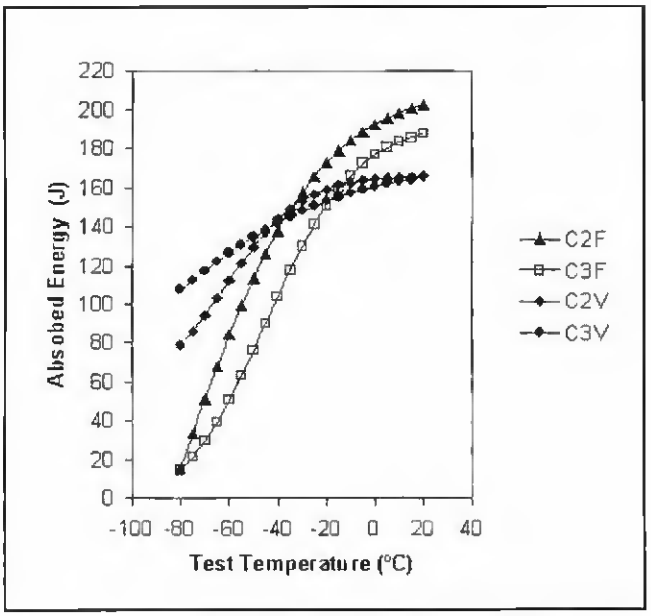

Fig. 6 — Charpy-V notch impact results for all-weld-metals CO_2 protection.

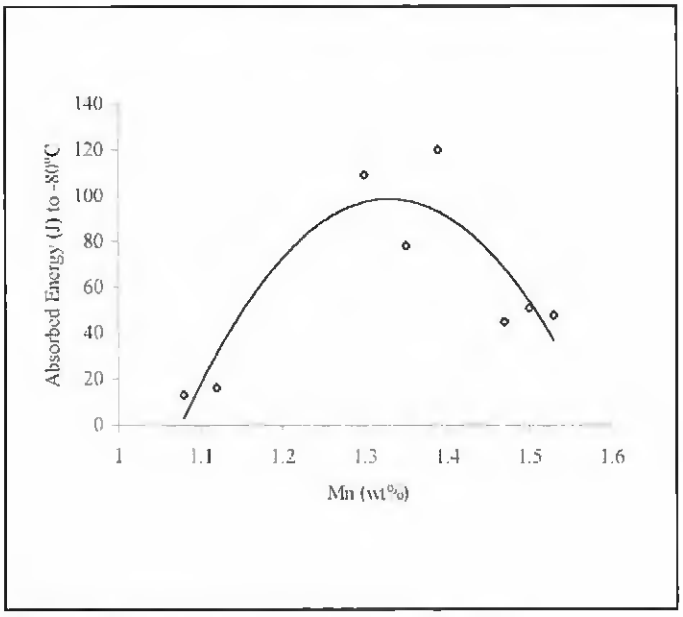

Fig. 7 — Absorbed energy at –80°C vs. manganese content.

cored wires creates less fume and spatter. *Welding Journal* (74)12: 45–49.

3) Sakai, Y., Aida, G., Suga, T., and Nakano, T. 1989. Development of various flux-cored wires and their application in Japan. IIW/IIS Doc. XII-1131-89.

4) Sakai, Y., Aida, G., Suga, T., and Nakano, T. 1989. Metal type flux-cored wire for carbon steel IIW/IIS Doc. XII-1131-89.

5) Lathhabai, S., and Stout, R. D. 1985. Shielding gas and heat input effects on flux cored weld metal properties. *Welding Journal* 64(11): 303-s to 313-s.

6) Myers, D. 2002. Metal cored wires: advantages and disadvantages. *Welding Journal* 81(9): 39–42.

7. Huisman, M. D. 1996. Flux and metal-cored wires, a productive alternative to stick electrodes and solid wires. *Svetsaren* 51(1–2): 6–14.

8. Schumann, G. O., and French, I. E. 1995. The influence of welding variables on weld metal mechanical and microstructural properties from conventional and microalloyed rutile flux-cored wires. Australian Welding Research. *CRC* 8(6): 1–12.

9. Vercesi, J., and Surian, E. 1996. The effect of welding parameters on high-strength SMAW all-weld-metal — Part 1: AWS E11018M. *Welding Journal* 75(6): 191-s to 196-s.

10. Vercesi, J., and Surian, E. 1997. The effect of welding parameters on high-strength SMAW all-weld-metal — Part 2: AWS E10018M and E12018M. *Welding Journal* 77(4): 164-s to 171-s.

11. Gianetto, J. A., Smith, N. J., McGrath, J. T., and Bowker, J. T. 1992. Effect of composition and energy input on structure and properties of high-strength weld metals. *Welding Journal* 71(11): 407-s to 419-s.

12. Strunck, S. S., and Stout, R. D. 1972. Heat treatment effects in multi-pass weldments of a high-strength steel. *Welding Journal* 51(10): 508-s to 520-s.

13. Glover, A. G., McGrath, J. T., Tinkler, M. J., and Weatherly, G. C. 1977. The influence of cooling rate and composition on weld metal microstructures in a C/Mn and a HSLA steels. *Welding Journal* 56(9): 267-s to 273-s.

14. Dorschu, K. E. 1968. Control of cooling rates in steel weld metal. *Welding Journal* 47(2): 49-s to 62-s.

15. Vaidya, V. 2002. Shielding gas mixtures for semiautomatic welds. *Welding Journal* 81 (9): 43–48.

16. Evans, G. M. 1982. Effect of welding position on the microstructure and properties of C-Mn all-weld metal deposits. *Welding Review* 1(3): 6–10. *Welding Res. Abroad* 1983. 29(1): 46–57.

17. ANSI/AWS A5.29-98. 1998. *Specification for Low-Alloy Steel Electrodes for Flux Cored Arc Welding*. Miami, Fla.: American Welding Society.

18. Schnadt, H. M., and Leinhard, E. W. 1963. Experimental investigation of the sharp-notch behavior of 60 steels at different temperature and strain rates. IIW-IIS Doc. 196-343-63.

19. Guide to the light microscope examination of ferrite steel weld metals. IIW Doc. IX-1533-88. 1988.

20. *Standard Test Methods for Determining Average Grain Size*. 1996. ASTM E112-96e1.

21. Evans, G. M. 1982. Effect of heat input on the microstructure and properties of C-Mn all-weld metal deposits. *Welding Journal* 61(4):125-s to 132-s. *Welding Research Abroad*. 1983. 29(1): 35.

22. Ramini de Rissone, N. M., Souza Bott, I. de, Vedia, A. de, and Surian, E. 2001. The effect of welding procedure ANSI/AWS A5.20-95 E71T1 flux cored wire deposits. Paper presented at AWS Annual Meeting, April, Detroit, Mich. *STWJ* 8 (2): 113–122.

23. Ferrante, M., and Farrar, R. A., 1982. The role of oxygen rich inclusions in determining the microstructure of weld metal deposits. *Journal of Materials Science* 17: 3293–3298.

24. Babu, S. S., David, S. A., Vitek, J. M., Mundra, K., and DeBroy, T. Development of macro- and microstructures of carbon-manganese low alloy steel welds: Inclusion formation. *Material Science and Technology* 11: 186–199.

25. Evans, G. M. 1991. Effect of nickel on the microstructure and properties of C-Mn all-weld deposits. *Joining Sciences* 1(1): 2s-13s. 1991, *Welding Res. Abroad* 37(2/3): 70–83, IIS-IIW Doc II-A-791-89, 1989, *Schweissmitteilungen* 48(122): 18–35 1990.